A SPECULAR MODEL FOR UVGI AIR DISINFECTION SYSTEMS

W. J. KOWALSKI,* W. P. BAHNFLETH, AND R. G. MISTRICK

Department of Architectural Engineering Department, The Pennsylvania State University, Engineering Unit A, University Park, PA 16802 * Corresponding Author: Email: drkowalski@psu.edu

ABSTRACT

A model for predicting the ultraviolet (UV) irradiance field inside specularly reflective rectangular ultraviolet germicidal irradiation (UVGI) air disinfection systems is developed based on a view factor model of the UV lamps and a virtual image model of the specular reflections. The combined three-dimensional irradiance field, direct and reflective, is used to estimate the UV dose absorbed by airborne microorganisms in mixed air. Predicted inactivation rates are then compared with existing bioassay test data for the microorganisms *Serratia marcescens, Bacillus subtilis spores, Staphylococcus epidermis,* and *Mycobacterium parafortuitum*. A dimensionless analysis is performed using quantitative results of the computer model. Some conclusions are drawn regarding the design and optimization of UVGI air disinfection systems. Differences between this model and a diffusive model of reflectivity are discussed.

INTRODUCTION

Ultraviolet radiation in the range of 225–365 nm is highly lethal to many microorganisms, especially viruses and bacteria. Air disinfection systems using UVGI have been in use for over seventy years but until recently, no detailed modeling tools were available to analyze the three-dimensional (3D) irradiance field and predict inactivation rates for airborne microbes. Previous methods for sizing UVGI systems have involved variations of the inverse square law or the line source inverse square law, but these models are unable to accurately predict the near field irradiance or the far field irradiance of UV lamps to the precision necessary for air disinfection applications. These methods may have proved effective for UVGI disinfection of water, but irradiation of water is highly dependent on near field absorbance (Severin et al. 1983). Since the absorbance of UV in air is negligible and the size of air disinfection systems typically involves distances of up to one meter or more, there is a need for higher precision than can be achieved with most previous methods.

The specular model presented here builds on the authors' previous research into UVGI lamp models based on view factors. The new model includes the same view factor lamp model but replaces the diffuse reflectivity model with a specular virtual image model. Although the previous diffuse reflectivity model provided good agreement with laboratory data, it included various assumptions. The present specular model includes no assumptions other than that the surface is purely specular, that is, that the reflective surfaces produce mirror-like virtual images of the lamp. In actuality, reflective surfaces are partly specular and partly diffuse, and therefore an ideal model would use both specular and diffuse components. The purpose of this research, however, is to address specular reflectivity only.

In addition to presenting the new specular model, this paper re-addresses laboratory data previously used to justify the diffuse model. It also summarizes the exponential decay curve for microbial exposure to UV irradiation and provides a summary of the dimensionless analysis of rectangular UVGI specular systems.

Thermal radiation view factors can provide considerably more realistic models of UV lamp irradiance fields than previous methods (Kowalski and Bahnfleth 2000). A view factor model of a lamp as a cylinder can provide more accuracy in the near field and far field than any form of the inverse square law and the use of such a model to predict lamp irradiance at any distance provides superior agreement with photosensor readings (Kowalski et al. 2000). A previous model of UVGI systems using a view factor for the lamp and a separate view factor for the reflective enclosure surfaces had good success predicting inactivation rates of airborne microbes based on laboratory tests (Kowalski 2001). However, view factors define only diffuse surfaces, which are adequate for lamps, but can only accurately depict diffusely reflective surfaces. This paper addresses specularly reflective surfaces and models them using a geometric method based on virtual lamp images. This method applies to rectangular UVGI air disinfection systems such as shown in Figure 1.

The placement of the lamp shown in Figure 1 is orthogonal to the x axis but this model can easily be applied to lamps oriented in any axis or at non-orthogonal angles. For simplicity's sake, however, this paper only addresses the condition in which flow is along the z axis, the lamp is orthogonal to the x axis, and the lamp has one end at $x = 0$.

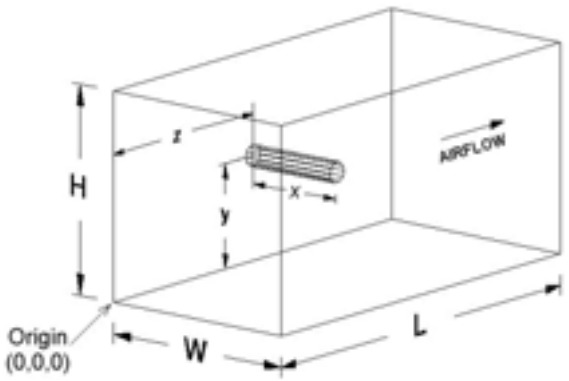

Figure 1: Layout of a rectangular UVGI system showing outside dimensions (W, H, & L) and the lamp coordinate reference system (*x*, *y*, and *z*).

THE VIEW FACTOR LAMP MODEL

The view factor model of the lamp has been previously developed (Kowalski et al 2000; Kowalski 2001) and is used to define the irradiance produced at any point inside the UVGI enclosure (see Figure 1) and is recapitulated here. The following view factor will define the fraction of radiative intensity leaving cylindrical area 2 that arrives at differential area 1 (Modest 1993):

[1] $$F = \frac{L}{\pi H}\left[\frac{1}{L}\tan^{-1}\left(\frac{L}{\sqrt{H^2-1}}\right)+\frac{X-2H}{\sqrt{XY}}\tan^{-1}\left(P\sqrt{\frac{X}{Y}}\right)-\tan^{-1}P\right]$$

The parameters in the above equation are defined as follows:

[2] $$H = x/r$$

[3] $$L = \ell/r$$

[4] $$X = (1+H)^2 + L^2$$

[5] $$Y = (1-H^2) + L^2$$

[6] $$P = \sqrt{\frac{H-1}{H+1}}$$

In equations 1 through 6

ℓ = length of the lamp segment, cm
x = distance from the lamp, cm
r = radius of the lamp, cm

This equation applies to a differential element located at the edge of the cylindrical lamp segment. In order to compute the irradiance field at any point along the axis of the lamp and at any distance from the axis, the lamp must be modeled in two parts of lengths ℓ_1 and ℓ_2. The following relation will then describe the total irradiance field from the two segments:

[7] $$F_{tot}(x,\ell) = F_1(x,\ell_1) + F_2(x,\ell_2)$$

where ℓ_1 = length of lamp segment 1, cm
ℓ_2 = length of lamp segment 2, cm

The irradiance at any point from the lamp surface defined by a distance from the axis and a distance along the lamp length (from one end) is computed by multiplying equation 7 by the surface irradiance of the lamp. The surface irradiance is computed from the UV power output and the resulting equation is:

[8] $$E(x,\ell) = \frac{P_{uv}}{2\pi r\ell}\left[F_1(x,\ell_1) + F_2(x,\ell_2)\right]$$

where $E(x,\ell)$ = UV irradiance at any point from lamp surface, μW/cm^2
P_{uv} = UV radiant power output of the lamp, μW

The accuracy of equation 8 depends on the accuracy to which the UV lamp power output P_{uv} is known, and many of these have been tabulated or are available from lamp manufacturers (IESNA 2000). For details on computing the irradiance at points beyond the end of the lamp, refer to Kowalski and Bahnfleth (2000) or Kowalski (2003).

The view factor in equation 1 considers the receiving surface to be oriented facing the cylindrical lamp axis no matter where the surface is located in space. It is assumed that airborne microbes are spherical and will, therefore, always present a circular profile to the UV lamp. The virtual images of the UV lamps, since they are also modeled by equation 1, carry the same implication. This view factor approach may not be a perfect definition of the reality of microbial exposure, since it ignores the possibility of refraction at the surface of the microbe, but it is a reasonable first approximation in lieu of future data to the contrary.

THE VIRTUAL IMAGE MODEL

The model developed in this study uses a single view factor to define the lamp irradiance field, and then uses multiple virtual images of the lamp to compute the reflected irradiance field. The virtual images are treated as separate lamps with lower UV power. The cylindrical view factor is applied to the lamps images at their virtual distance and their UV power output is reduced by the reflectivity of each surface the image passes through. For example, a lamp that is 10 cm from a 90% specular reflective surface has a virtual image 10 cm on the other side of the reflective surface, and the effective UV power of that virtual image is 90% of the real lamp UV power. Figure 2 illustrates the virtual image of a lamp in a single specular reflective surface.

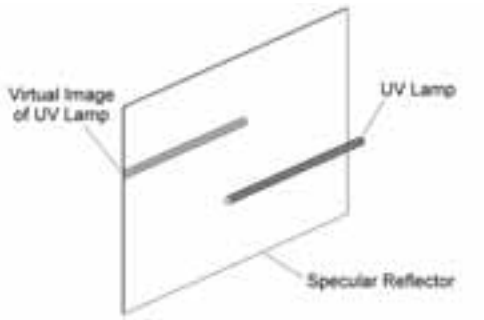

Figure 2. A specular reflector (mirror) will show a virtual image of the real lamp an equivalent distance behind the reflector surface.

Figure 3 shows a photograph of a rectangular UVGI system with one-way mirrors in which at least six virtual images of a single UV lamp can be seen reflected in the rectangular surfaces.

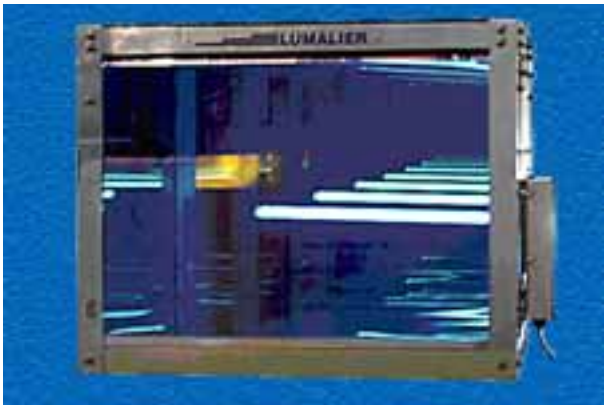

Figure 3. UVGI System made from one-way mirrors. At least six virtual images can be seen in this photograph. Photograph provided courtesy of Lumalier.

Figure 4 illustrates the model in terms of the real lamp in the center and the virtual images of the first two reflections. In the model used here, sixty virtual lamps are used covering the first five reflections. Contributions for reflections beyond the first five tend to be negligible, even for very high reflectivity, due primarily to the distances involved. It is possible, however, that the contribution can be significant for small systems with high reflectivity. The number of reflections has been limited in this model due to the amount of computation time required.

In mathematical terms, the reflected images provide contributions to the irradiance at a point as per the following:

[9] $$E_{uv} = \frac{P_{uv}}{2\pi r^2} F_0 + \frac{\rho P_{uv}}{2\pi r^2} F_1 + \frac{\rho^2 P_{uv}}{2\pi r^2} F_2 + \ldots$$

Figure 4. Schematic of the virtual image array showing the real lamp, the four first reflection images (1), the eight second reflection images (2), and a ring of third reflection images.

where F_0 = direct irradiance contribution from UV lamp
F_1 = irradiance contribution from all first reflections
F_2 = irradiance contribution from all second reflections

Equation 9 can be simplified as:

[10] $$E_{uv} = \frac{P_{uv}}{2\pi r^2}\left[F_0 + \rho F_1 + \rho^2 F_2 + \ldots\right]$$

Figure 5 shows some example results for the average irradiance fields caused by each of the first five virtual lamp images.

UVGI INACTIVATION RATES

The inactivation rates due to UVGI exposure are based on the classic single stage logarithmic decay equation:

[11] $$\ln S = -kE_{avg}t$$

where S = Survival fraction of population
k = UVGI rate constant, cm²/μJ
E_{avg} = average UVGI irradiance, μW/cm²
t = exposure time

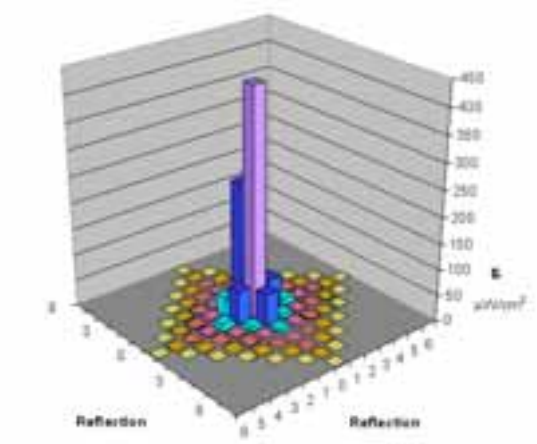

Figure 5. Irradiance contributions from virtual reflected lamp images. The tall bar in the center represents the direct lamp irradiance contribution.

The average irradiance in equation 11 is defined by the exposure to which the microbe is subject. In plate-based experiments, the irradiance is the radiative flux on the surface of the plate. In airborne experiments the irradiance is the spherical irradiance. It should be noted here that the term irradiance is used in accordance with current usage but that, in fact, the more technically correct term is 'fluence rate', since it refers to the irradiance passing through the entire surface of the airborne microbe modeled as an infinitesimal sphere. Insufficient data is available to determine how significant the differences are between rate constants predicted by airborne vs. plate-based tests, but the data that does exist suggests they are within a single order of magnitude (Kowalski et al 2000).

The inactivation rate, IR, is simply the complement of the survival rate, or:

[12] $$IR = 1 - e^{-kE_{avg}t}$$

The UVGI dose is defined as the average irradiance multiplied by the exposure time. When the dose is low for resistant microbes like spores, there tends to be a two stage decay curve. That is, a resistant fraction of the microbial population behaves as if it were a second species and the

population reduction occurs at a slower rate (i.e., a lower rate constant).

The application of equation 12 carries the assumption of uniform air mixing. In the case of unmixed air the inactivation rate must be computed for each and every point in a three-dimensional (3D) matrix defining the enclosure volume. This latter approach will invariably produce inactivation rates that are lower than the mixed air case due to inefficiencies that are associated with local extremes in the irradiance fields. Evidence suggests that complete mixing is more likely to be the case in any real world UVGI system (Severin et al. 1983). A practical approach, and the one used here, is to use both the unmixed air condition and the mixed air condition to define a range of inactivation rates.

BIOASSAY TEST RESULTS

Table 1 summarizes the results of some 32 tests on four different microbes. Three separate laboratories performed these tests. The bioassay inactivation rate in the final column is compared against the predicted inactivation rates of the program. The predicted inactivation rates are shown in terms of the range between the unmixed air condition and the mixed air condition. In the unmixed air condition the streamlines are considered parallel. In the mixed air condition the entire microbial population is assumed to be exposed to the same average irradiance inside the enclosure. The overall average range of predicted inactivation rates for all microbes is 57 – 78% and the average measured inactivation rate is 76%.

Figure 6 displays the results of Table 1. Two data sets that produced bioassay inactivation rates of approximately zero percent for *B. subtilis* spores were not included in Figure 5 or Table 1. The B. *subtilis* test results show two bioassays each from two different laboratories. Results from the separate labs gave different results and it was not possible to rectify them. The second two *B. subtilis* data points are based on a two stage decay model.

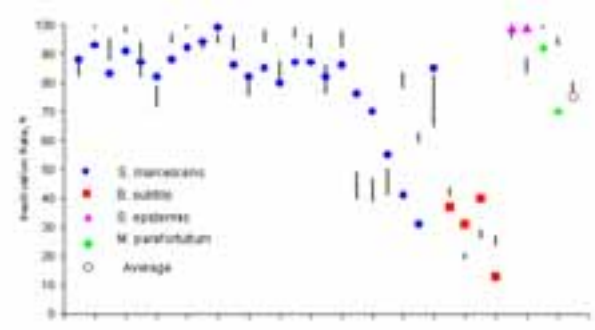

Figure 6. Range of Predictions vs. Bioassay Test Results.

Two additional bioassay test results for *S. marcescens* were excluded due to gross deviations that were anomalous and which were believed due to incorrectly stated reflection coefficients that could not be verified. Two additional data sets for *S. marcescens* that appeared to be anomalous were included, since it was not clear that any laboratory error had been made. The latter are the twentieth and twenty-first data sets in Table 1 and Figure 6.

Table 2 summarizes the rate constants used in the previous test result comparisons (UVDI 2000, 2002). The rate constant for *S. marcescens* was computed based on the test results themselves and is similar to that produced by other studies (Collins 1971, Peccia et al. 2001). The rate constant for *B. subtilis* spores is based on the average of the five indicated studies. The rate constant for *M. parafortuitum* is based on a normal indoor relative humidity range of 70-80%.

Table 2. Rate Constants for Test Bacteria

Microorganism	UVGI Rate Constant $cm^2/\mu J$	Source
S. marcescens	0.002909	UVDI 2000
B. subtilis spores	0.000324	Sharp 1939
B. subtilis spores (multi-hit model)	0.0001529	Nagy 1964; Chang et al. 1985; Nakamura 1987; Sommer et al. 1989, 1995 (average)
S. epidermis	0.0008372	Harris et al. 1993
M. parafortuitum	0.00135	Peccia, et al. 2001

DIMENSIONLESS PARAMETER COMPARISONS

The performance of rectangular UVGI air disinfection systems can be defined with a set of variables describing enclosure geometry, lamp characteristics, airflow conditions, and characteristics of the microbe. Table 3 lists the critical variables and units that define the inactivation rate of rectangular UVGI systems. The flow rate Q effectively defines the air velocity and the exposure time, in combination with the dimensions, and therefore these factors are redundant.

Some variables that may be important to the disinfection process are not yet well understood or sufficiently quantified to be useful, such as the effects of photoreactivation rate, temperature, and relative humidity on microbial rateconstants. The temperature and air velocity may also impact the performance of individual manufacturers' lamps. The latter effects cannot be generalized but the UV power for the lamp will usually include the effect of these parameters when they are known from manufacturer's information or when lamp operating conditions are defined by a design velocity and temperature range.

Table 1: Summary of Bioassay Results vs. Program Predictions

						% Inactivation Rate	
Test Microbe	HxWxL (cm)	Airflow m^3/min	ρ %	UV Power (W)	Average *E* ($\mu W/cm^2$)	Mixed-Unmixed	Bioassay
S. marcescens	46x46x188	34	7	11.78	1063	83 - 88	88
	46x46x188	34	7	34.77	3136	99 - 99.8	93
	30x64x91	85	7	35.76	2219	88 - 96	83
	46x46x183	34	7	28.35	2556	98 - 99	91
	46x46x183	34	7	17.34	1456	83 - 94	87
	46x46x183	34	7	8.94	792	72 - 79	82
	46x46x183	51	7	29.16	2629	94 - 97	88
	46x46x183	34	7	36.51	3316	99 - 99.9	92
	46x46x183	57	7	29.37	2648	92 - 96	94
	46x46x183	57	7	64.08	2909	94 - 97	99
	30x64x91	57	57	17.56	6091	91 - 96	86
	30x64x91	57	57	9.05	3160	76 - 82	82
	30x64x91	57	57	21.82	7534	94 - 98	85
	30x64x91	57	57	11.07	3848	81 - 88	80
	25x64x91	40	57	19.01	7480	96 - 99	87
	30x64x91	57	57	18.13	6436	92 - 97	87
	30x64x91	57	57	8.35	3600	77 - 86	82
	30x64x91	57	57	16.75	7187	92 - 98	86
	30x64x91	57	57	4.18	1237	40 - 49	76
	30x64x91	57	57	3.83	1161	39 - 47	70
	30x64x91	57	57	5.7	1287	41 - 50	55
	30x64x91	57	57	10.6	3320	79 - 84	41
	30x64x91	57	57	5.8	1817	59 - 63	31
	30x64x91	57	57	21.52	3216	65 - 83	85
B. subtilis spores	30x64x91	57	57	24	9405	41 - 44	37
	30x64x91	57	57	24	3883	19 - 21	31
	30x64x91	28.3	22	36	1473	26 - 29	40
	30x64x91	28.3	22	18	2695	24 - 27	12.8
S. epidermis	30x64x91	28.3	22	36	1473	96 - 98	99
	30x64x91	28.3	22	18	826	84 - 89	99
M. parafortuitum	30x64x91	28.3	22	58.32	2886	99 - 99.8	92
	30x64x91	28.3	22	29.16	1497	93 - 96	70

Table 3. Critical Parameters of Rectangular UVGI Systems

Parameter	Description	Units
W	Duct Width	cm
H	Duct Height	cm
L	Duct Length	cm
r	Lamp Radius	cm
ℓ	Lamp Arc Length = x, the lamp end coordinate	cm
P	Lamp UV Radiant Power	μW
Q	Air Flow Rate	m^3/min
x	Lamp end coordinate (= lamp arc length with base at *x* = 0)	cm
y	Lamp Y position or distance above bottom surface	cm
z	Lamp Z position or distance from duct entrance	cm
k	UVGI Rate Constant	$cm^2/\mu J$
ρ	Surface reflection coefficient	---

Previous research has identified ten dimensionless parameters that define the performance of rectangular UVGI systems (Kowalski et al. 2003). Table 4 lists these parameters and their typical range.

Table 4. UVGI Dimensionless Parameters

Parameter	**Description**	**Typical Range**
W/H	Aspect Ratio	1–4
r/ℓ	Lamp aspect Ratio	---
kPL/Q	Specific UV Dose	~1–2
x/W	X Ratio	<0.25 or >0.75
y/H	Y Ratio	>2*r*
z/L	Z Ratio	0.5
H/L	Height Ratio	0.25–10
ρ	Surface reflection coefficient	0.50–0.99

These dimensionless parameters provide a convenient means of studying the performance of UVGI systems in a quantitative way. These dimensionless parameters have been found to have negligible interaction in most cases, and minor interaction in only a couple of cases (Kowalski et al. 2003). This fact allows the parameters to be compared on a one-to-one basis to observe their behavior.

Each parameter can be compared with each other by computing the performance of specular UVGI systems for 100 cases that represent the range of dimensionless parameters shown in Table 4. Several thousand computer runs were used to evaluate all possible combinations of the dimensionless parameters, and the most important or representative results are summarized here. The results are plotted in 10x10 contours and discussed following.

Figure 7 shows a comparison of the inactivation rates predicted for the dimensionless parameters of the duct aspect ratio (*W/H*) vs. the specific UV dose (*kPL/Q*). It can be observed that as the specific UV dose in increased the inactivation rate increases in an exponential fashion and approaches a 100% inactivation rate asymptotically. This is true regardless of which parameter it is compared against due to a lack of interaction. The duct aspect ratio is observed to have a slight dip when the duct is square, *W/H* = 1.0, or to produce higher inactivation rates when the duct aspect ratio is above approximately 2.0.

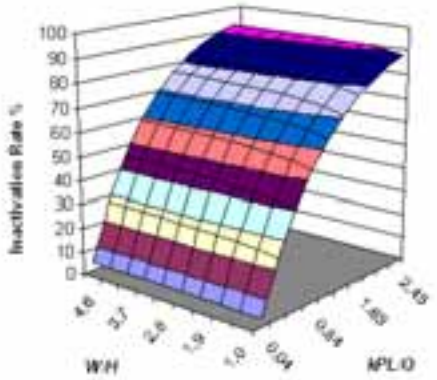

Figure 7. Duct Aspect Ratio vs. Specific UV Dose.

Figure 8 shows the X ratio (*x/W*) vs. the duct aspect ratio (*W/H*). It can be seen that the duct aspect ratio produces the highest inactivation rates when the width is twice the height or greater. This is, of course, for lamps that are parallel to the width. This is true regardless of what parameter the duct aspect ratio is plotted against since there is negligible interaction between these terms. The X ratio, which is the lamp length over the duct width, produces maximum inactivation rates at values near 1, or when the lamp spans the full length of the duct. It can be observed that the curve for the X ratio is slightly bi-modal and has a slight discontinuity near the value of 0.5 (when the lamp is centered). This is true regardless of the parameter the X ratio is plotted against and can be explained, at least theoretically, in terms of the fact that as the length of the lamp exceeds half the width, the contribution of the opposite reflective surface becomes more significant.

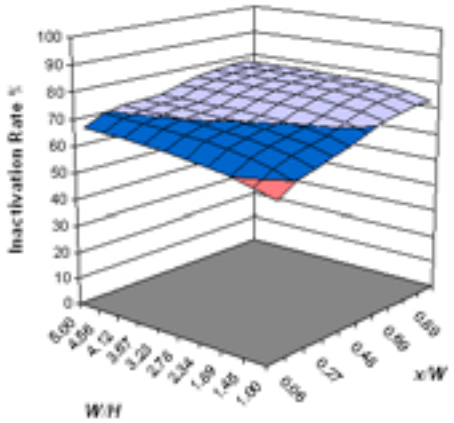

Figure 8: Duct Aspect ratio vs. X Ratio.

Figure 9 graphs the specific UV dose vs. the reflectivity. The reflectivity produces an approximately linear increase in inactivation rates only up to a point, since the inactivation rates cannot exceed 100%. The specific UV dose causes an approximately exponential increase in inactivation rates but again only until the inactivation rates approach 100%. It can be theorized that there must exist some optimum combination of UV power and reflectivity that maximizes inactivation rate and minimizes cost for any given UVGI system, but this result will depend on a full economic evaluation and economics are not addressed here.

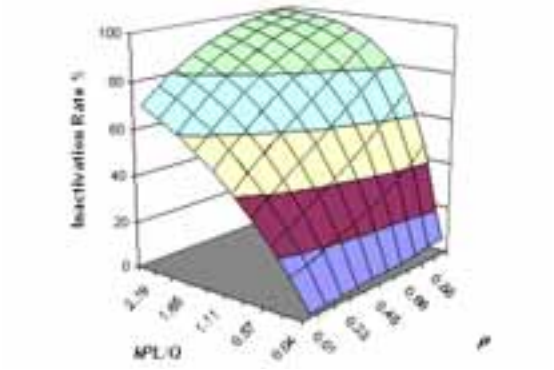

Figure 9: Reflectivity vs. Specific Dose.

Figure 10 shows the duct aspect ratio plotted against the Z ratio. The duct aspect ratio is optimum at values of approximately 2 or greater, as seen in previous charts. The Z ratio represents the depth within the duct that the lamp is located. It is clear that the optimum location of the lamp is a value of 0.5, or centered within the duct depth. This is, of course, rather intuitive and also represents common practice.

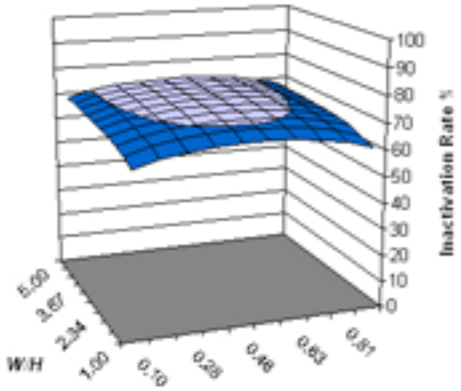

Figure 10: Duct Aspect Ratio vs. Z Ratio.

Figure 11 shows the reflectivity plotted against the duct aspect ratio. For both these parameters the chart shows the same characteristics seen previously. Reflectivity causes a nearly linear increase in inactivation rates while the optimum duct aspect ratio occurs at values somewhat above 2.

Figure 11: Reflectivity vs. Duct Aspect Ratio.

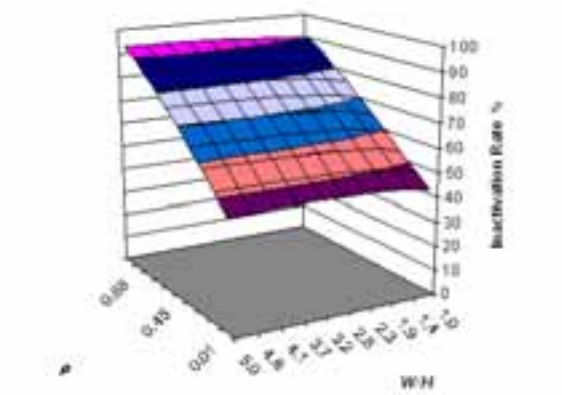

The lamp aspect ratio (r/l) has a negligible impact on inactivation rates and this is true in all cases and so no graphs are provided. No further contours need be shown since all the remaining combinations of parameters produce the same essential features shown in the previous graphs. That is, since there is negligible interaction, all the remaining contours are merely repetitions of the ones previously shown.

SPECULAR VS. DIFFUSE REFLECTIVITY

Although a previous model for diffusely reflective surfaces has been developed, the bases of these models are too different to allow valid direct comparison. The specular model tends to produce higher overall predictions of average irradiance fields but not in all cases. Both the diffuse and the specular models had predictive accuracies of approximately ±30% in over 90% of cases tested, although the differences in individual test results could vary widely between the models (approximately ±10%) and the diffuse model was slightly more accurate overall. The specular model yielded conclusions regarding lamp placement that vary considerably from the diffuse model. Further research is necessary to verify the irradiance field predictions of both these models before definitive conclusions can be drawn regarding the superiority of either type of surface reflectivity, but the simplicity of the specular model leaves less room for error than the more complex diffusive model. Research is also needed to combine these models to produce one that would incorporate partly diffuse, partly specular real-world reflective surfaces.

CONCLUSIONS

A specular model of UVGI systems has been summarized in which a view factor model of a UV lamp is used to create virtual images of the lamp and compute the irradiance field inside rectangular enclosures. Predictions of the model have been compared with 32 sets of test data and yield a predictive error of approximately ±30% in over 90% of test cases. Computer modeling results are presented in terms of dimensionless parameter comparisons. These comparisons suggest the following conditions may produce optimum inactivation rates for specular reflective systems:

- The duct aspect ratio should be greater than 2.
- The lamp should be centrally located along the depth of the duct.
- The lamp should be located at mid height in the duct.
- The lamp arc length should preferably span the duct width.

An interesting and possibly useful corollary of the dimensional analysis is the fact that the dimensionless parameters most critical in determining inactivation rates are the specific UV dose and the reflectivity. Combining these and rearranging a hypothetical function can be written to predict the UV power for any desired inactivation rate as follows:

[13] $$P = C\frac{Q}{\rho k L}$$

where C is some constant. If one assumes a constant reflectivity (i.e., 50%) and a standard rate constant (i.e., *Serratia*), it can be seen that the UV power is a linear function of the airflow per unit length of duct, for any given inactivation rate (i.e., 90%). This will only be true if the system is well designed in accordance with the above conditions and the inactivation rate is not extreme (i.e., in a shoulder or second stage region of the decay curve). Furthermore, this is merely an estimate of the UV power subject to the same error of the analysis (±30%) and is not a substitute for a detailed analysis of all factors.

No conclusions can be drawn regarding the benefits of specular versus diffusive reflective surfaces due to the fact that the models are merely approximations of the UV irradiance fields and, for reasons that are not yet clear, results do not corroborate well. The specular model predicts higher overall levels of irradiance than the diffusive model, but the diffusive model produces more accurate predictions of inactivation rates. Further research is needed to verify the irradiance field predictions of both the specular model and the previous diffusive model. Since the irradiance field predictions are, in fact, fluence rate predictions for spherical microbes, corroboration through testing may have to await perfection of the technology of spherical actinometry (Rahn et al. 1999).

Further conclusions regarding optimization of performance depend on the economics of UVGI systems and these matters remain to be addressed by future research. Additional research that remains to be performed includes further study of the effects of relative humidity and the photoreactivation effect. Other research needed for a complete description of UVGI system performance includes study of alternate geometries and lamp orientations, and the effect of reflective surfaces that are part diffusive and part specular. Ultimately, this research should lead to new guidelines for designing UVGI systems that have predictable performance in applications and that are energy efficient.

REFERENCES

Chang, J.C.H., Ossoff, S.F., Lobe, D.C., Dorfman, M.H., Dumais, C.M., Qualls, R.G., and Johnson, J.D. 1985. UV inactivation of pathogenic and indicator microorganisms. Appl. Environ. Microbiol. 49(6): 1361-1365.

Collins, F.M. 1971. Relative susceptibility of acid-fast and non-acid fast bacteria to ultraviolet light. Appl. Microbiol. 21: 411-413.

Harris, M.G., Fluss, L., Lem, A., and Leong, H. 1993. Ultraviolet désinfection of contact lenses. Optom. Vis. Sci. 70(10): 839-842.

IESNA 2000. Lighting Handbook, 9th Edition IESNA HB-9-2000. Illumination Engineering Society of North America, New York.

Kowalski, W.J., and Bahnfleth, W.P. 2000. Effective UVGI system design through improved modeling. ASHRAE Transactions 106(2): 4-15. http://www.engr.psu.edu/ae/iec/abe/publications/uvgi_system_design.pdf.

Kowalski, W.J., Bahnfleth, W.P., Witham, D.L., Severin, B.F., and Whittam, T.S. 2000. Mathematical modeling of UVGI for air disinfection. Quantitative Microbiology 2(3): 249-270. http://www.kluweronline.com/issn/1388-3593.

Kowalski, W.J. 2001. Design and optimization of UVGI air disinfection systems, PhD Thesis, The Pennsylvania State University, State College. http://etda.libraries.psu.edu/theses/available/etd-0622101-204046/.

Kowalski, W.J., Bahnfleth, W.P., and Rosenberger, J.L. 2003. Dimensional Analysis of UVGI Air Disinfection Systems. Intl. J. HVAC & R Research 9(3): 17.

Kowalski, W.J. 2003. Immune Building Systems Technology. McGraw-Hill, New York.

Modest, M.F. 1993. Nagy, R. 1964. Application and measurement of ultraviolet radiation.

Nagy, R. 1964. Application and measurement of ultraviolet radiation. AIHA J. 25: 274-281.

Nakamura, H. 1987. Sterilization efficacy of ultraviolet irradiation on microbial aerosols under dynamic airflow by experimental air conditioning systems. Bull. Tokyo Med. Dent. Univ. 34(2): 25-40.

Peccia, J., Werth, H.M., Miller, S., and Hernandez, M. 2001. Effects of relative humidity on the ultraviolet induced inactiva-tion of airborne bacteria. Aerosol Sci. Technol. 35: 728-740.

Rahn, R.O., Xu, P., and Miller, S.L. 1999. Dosimetry of room-air germicidal (254 nm) radiation using spherical actinometry. Photochem. Photobiol. 70(3): 314-318.

Severin, B.F., Suidan, M.T., and Englebrecht, R.S. 1983. Kinetic modeling of U.V. disinfection of water. Wat. Res. 17(11): 1669-1678.

Sharp, G. 1939. The lethal action of short ultraviolet rays on several common pathogenic bacteria. J. Bact. 37: 447-459.

Sommer, R., Weber, G., Cabaj, A., Wekerle, J., Keck, G., and Schauberger, G. 1989. UV-inactivation of microorganisms in water. Zentralbl. Hyg. Umweltmed 189(3): 214-224.

Sommer, R., Cabaj, A., Schoenen, D., Gebel, J., Kolsch, E., and Havalaar, A.H. 1995. Comparison of three laboratory devices for UV-inactivation of microorganisms. Wat. Sci. Technol. 31: 147-156.

UVDI 2000. Report on Bioassays of S. marcescens and B. subtilis exposed to UV irradiation. Ultraviolet Devices, Inc., Valencia, CA.

UVDI 2002. Report on Bioassay results for three microorganisms, Ultraviolet Devices, Inc., Valencia, CA.